Evidence against dust-mediated control of glacial-interglacial changes in atmospheric CO_2

Maher, B.A.*, Dennis, P.F.

Centre for Environmental Magnetism and Palaeomagnetism (CEMP) and Stable Isotope Laboratory, School of Environmental Sciences, University of East Anglia, Norwich NR4 7TJ

*Now at CEMP, Lancaster Environment Centre, Department of Geography, University of Lancaster, LA1 4YP

The 'iron fertilisation' hypothesis suggests controversially that atmospheric CO_2 has been influenced by transport of iron-containing dust to the ocean surface[1-3]. Experiments in the Southern Ocean show that productivity, and subsequent CO_2 drawdown, are enhanced by iron additions[4]. A carbon cycle model (forced by large values of Southern Ocean dust flux) indicates productivity changes during past glacial times could have reduced atmospheric CO_2 by ~40ppm [5]. However, Southern Ocean dust flux is very low at present and was increased, but still low, during past glaciations. Thus, as for the equatorial Pacific [1, 6, 7], distally-supplied, upwelled iron may be more significant than local dust-borne iron. Hence, Northern, not Southern, hemisphere dust may drive Southern Ocean productivity[8,9]. Here, we examine the flux and timing of N. Atlantic dust inputs in relation to the Vostok climate record. For the penultimate glaciation, two N. Atlantic dust peaks occurred. At 155 ka, the Atlantic dust flux was 2500x that at Vostok[10], but declined well before the onset of the Vostok CO_2 rise. The second

dust peak, at 130ka, substantially post-dated the CO_2 rise. Thus, low Southern Ocean dust fluxes, and this mismatch between N. hemisphere dust peaks and Southern Ocean climate change, appear not to support the suggested role of dust-mediated iron fertilisation in the Southern Ocean at Termination II.

The Southern Ocean is a 'high nutrient, low chlorophyll' (HNLC) region; phosphate and nitrate concentrations are high at the ocean surface yet its productivity is low. Recent experiments show that artificial additions of iron to ocean patches significantly enhance primary productivity [4], with consequent drawdown of surface water f(CO_2) - the water becoming a sink for atmospheric CO_2. Hence, the strength of the 'biological pump' may influence atmospheric CO_2 concentrations. The Vostok (Antarctic) ice core record shows that towards the end of past glacial stages, the Southern Ocean region warmed and atmospheric CO_2 levels rose several thousand years before the N. hemisphere ice sheets melted. Thus, this region may be critical for causing and/or amplifying climate change. A major control on iron supply to HNLC regions is thought to be the flux of terrestrial dust [5, 11]. To drive a model of the ocean-atmosphere carbon cycle, which predicts up to ~40 ppm CO_2 drawdown in response to increased Southern Ocean dust flux during glacial stages, Watson et al. [5] used a modelled estimate of modern dust flux, of 14 $mg.cm^{-2}.kyr^{-1}$ (a value which Mahowald et al. [12] themselves considered over-predicted) and an LGM value of 345 $mg.cm^{-2}.kyr^{-1}$. Data on the present-day dust flux to the Southern Ocean, whilst sparse, are mutually consistent [13, 14, 15] and indicate much lower fluxes of 0.1 – 1 $mg.cm^{-2}.kyr^{-1}$. At glacial times, increased aridity and/or wind strength could have contributed higher Southern Ocean dust fluxes and thus to lower atmospheric CO_2 concentrations. The Vostok record indeed shows peak dust flux during glaciations, when atmospheric CO_2 was depressed by ~80 ppm[16]. However, geological data indicate these increased glacial dust fluxes were small, and negligible compared with detrital (ie non-aeolian) sediment accumulation rates in the Southern Ocean. The Southern Ocean exhibits sedimentation

rates far greater than the atmospheric flux, due to bottom water-transport of detritus. For Scotia Sea sediments, for example, the aeolian contribution from the S. American loess regions (identified isotopically as the principal source of Vostok's dust[17]) is below the level of detection, even during glacial periods[18]. Similarly, in cores from the SE Indian Ocean to the Antarctic continental slope, aeolian particles account for <10 % of the clay minerals present[10]. An aeolian flux 600 x that actually recorded in the Vostok ice core (~ 2 $mg.cm^{-2}.kyr^{-1}$) would be required to explain the lithogenic flux at these sites during glacial times [10]. Thus, interpretation of lithogenic accumulation rates as a proxy for Southern Ocean dust flux [19] appears invalid. Similarly, dust concentration changes in the Vostok ice core cannot be used to constrain model simulations of past dust fluxes[5] because snow accumulation rates were lower during glacial stages; dust flux changes were hence much smaller than concentration changes[12].

Given the low dust fluxes to this region, iron supply from upwelling water appears a more significant source, by at least an order of magnitude [5, 8, 9]. Similar upwelled iron supply has been identified for the HNLC region of the equatorial Pacific [6, 7]. Thus, for the Southern Ocean, upwelled iron and resultant productivity may reflect distal (ie N. hemisphere), rather than S. hemisphere, dust inputs. It has been suggested that iron from the peri-Saharan region (the largest dust source in the world) may be transported in southward flow of the N. Atlantic intermediate/deep water to the circumpolar region, on a timescale of ~ 100 years [8]. This hypothesis suggests that the pattern of N., rather than S., hemisphere dust flux may match more closely the pattern and timing of CO_2 variations recorded by the Vostok ice core.

Here, we test this hypothesis by high-resolution oxygen isotope, magnetic and elemental analysis of a deep-sea sediment record, Core 82PCS01, from the abyssal plain northeast of the Azores. Sedimentation at this site has been continuous and undisturbed from oxygen isotope stage (OIS) 8 to the present day [20]. The core site lies above the

lysocline, precluding carbonate dissolution, and underlies the present-day northern margin of the Bermuda-Azores high pressure system, around which African dust can be transported northwards in the summer [21, cover photo]. Upon sinking, possible complexation or dissolution[22], iron may become entrained within southward-flowing Atlantic intermediate/deep water. We obtained an age model for the core via oxygen isotope analysis of the planktonic foraminifer, *Globorotalia bulloides*, correlating the data with Martinson et al.'s [23] chronostratigraphy. We measured the magnetic remanence acquired at high applied magnetic fields (the HIRM) of the sediments, as a proxy for iron. Additional analyses on subsets of samples included carbonate content, elemental iron and dry bulk density. From these data, we calculated sedimentation rates and fluxes of iron and dust.

Figure 1 shows the oxygen isotope data for Core 82PCS01, with the chronology based on tie points to the high-resolution chronostratigraphy of Martinson et al.[23]. Also shown in Figure 1 is the Vostok $\delta^{18}O$ (in air) record[16]. Both these chronologies agree strongly (to within 1 kyr) with that newly derived by tuning of the benthic marine $\delta^{18}O$ record (and the Vostok air $\delta^{18}O$ record) to tilt and precession cycles[24]. Figure 2 shows the $\delta^{18}O$ and HIRM data for Core 82PCS01, for the time interval 100 -180 ka. For comparison, terrigenous % data are also shown for another, more southerly core in the eastern Atlantic. Core 82PCS01 appears to record a representative (but much higher resolution) signal of dust input over at least a regional scale. For glacial stage 6, Core 82PCS01 displays two peaks in HIRM, at ~ 130 ka and ~155 ka. For the succeeding interglacial stage, from ~125 to 100 ka, HIRM values are low and less variable. These high-resolution data amplify those reported [25] for gravity cores in this area. Goethite, a significant component of soils within the semi-arid zone, has been identified as the major contributor to the HIRM of these sediments [25]. Given the saturation remanence of goethite[26] (~0.05 $A.m^2.kg^{-1}$), our carbonate-free HIRM values (7 – 44x

10^{-4} A.m^2.kg^{-1}) indicate goethite concentrations in the dust component of the sediment of 1.4 - 8.8 %. HIRM values (for every sample) and independently-determined iron (wt%, determined for a subset of samples) are directly and strongly correlated (R^2 = 0.83). Thus, rapid, non-destructive HIRM measurements appear to be a robust proxy for aeolian, elemental iron concentrations in these N. Atlantic sediments. It should be noted that our N. Atlantic record documents particulate iron deposition through time, rather than dissolved iron. The relationship between iron-bearing dust flux and dissolved iron concentrations in deep water is presently not known, but dust-sourced increases in deep water iron would imply increased concentrations of organic ligands capable of complexing the iron to maintain solubility[22].

Figure 3a shows the calculated dust fluxes for Core 82PCS01, for the period spanning glacial stage 6, Termination II and interglacial stage 5. Dust flux was 3 - 5 x higher during two intervals, ~ 155 ka (~5 g.cm^{-2}.kyr^{-1}) and ~ 130 ka (~3 g.cm^{-2}.kyr^{-1}). During interglacial stage 5 (from ~130 ka on), dust fluxes decreased rapidly before steadying at ~ 1 g.cm^{-2}.kyr^{-1}. For comparison, estimates of modern fluxes [12] for the NE equatorial Atlantic mostly range from 0.2 - 3 g.cm^{-2}.kyr^{-1}, with (depending on latitude) a one- to four-fold increase in dust flux at the Last Glacial Maximum.

The oxygen isotope records from 82PCS01 and Vostok are in excellent agreement (Figure 1). At Termination II, the rise in $\delta^{18}O$ (in air) at Vostok lags the N. Atlantic rise by ~2 ka, this delay attributable to the Dole effect [24]. The major, five-fold increase in our N. Atlantic dust flux is thus virtually synchronous with peak A in the Vostok dust concentration record (figure 3c). However, at its peak, the Vostok dust *flux* is ~2500 x smaller than our N. Atlantic flux (~2 mg.cm^{-2}.kyr^{-1} compared with 5 g.cm^{-2} kyr^{-1}). In global climate terms, this major rise and fall in N. Atlantic dust (and iron) flux occurred entirely within OIS 6, with little apparent variation in either atmospheric CO_2 or oxygen isotope values (figure 3d-g). N. Atlantic dust flux then declined, substantially

earlier (by ~7000 years) than the onset of the CO_2 rise at Vostok. The second dust flux event in Core 82PCS01, centred on ~130 ka, may have provided a significant, later supply of iron to drive Southern Ocean productivity, when S. hemisphere dust flux had diminished to near-zero. However, as shown in figure 3, this subsidiary peak in dust flux significantly post-dates (by ~7000 years) the onset of the CO_2 rise. Rather than being associated with drawdown of CO_2 and maintenance of glacial conditions, the peak of this later event coincides with a marked, ~1 $^{o}/_{oo}$ shift in oxygen isotope values (fig. 3d), indicating either warming N. Atlantic sea surface temperatures [27] and/or melting of the N. hemisphere ice sheets.

Thus, whilst fluxes of N. hemisphere dust may constitute an alternative, higher-magnitude supply of iron to the Southern Ocean, they seem to bear no causal relationship with either changes in Southern Ocean temperature or atmospheric CO_2, as recorded at Vostok around Termination II. These data - the evidence of very low dust fluxes to the Southern Ocean, and the mismatch of timing between the N. hemisphere flux peaks and Southern Ocean climate change - thus do not appear to support the suggested role of dust-mediated iron fertilisation in the Southern Ocean at and around the Termination II boundary.

Methods.

From each 1 cm sample (sieved at 63 μm), 10-20 adult specimens (0.2 to 0.5 mg) of the planktonic foraminifer, *Globorotalia bulloides*, were picked for oxygen isotope analysis. These were reacted off-line with 102% orthophosphoric acid at 25 ^{o}C for 12 hours, the evolved CO_2 dried by passing through a cold trap at –90 ^{o}C and cryodistilled into gas sample tubes. Isotopic analyses were performed on a VG SIRA series II dual inlet isotope ratio mass spectrometer. Oxygen isotopic compositions, with respect to the Vienna PDB (VPDB) standard, are accurate and precise to better than < 0.1‰. Analyses of 0.2 mg aliquots of the internal lab. standard run at random with the

foraminiferal samples, at an average frequency of 1 in 4 samples, have a precision ($1\sigma_{n-1}$) of ±0.06‰ (n = 30). For magnetic analysis, the < 63 μm fraction of each sample was dried and packed into 10 cc plastic cylinders. Magnetic fields were generated using a pulse magnetiser (up to 100 mT) and electromagnet (up to 1 T); magnetic remanences measured using a fluxgate magnetometer (sensitivity ~10^{-7} A m^2). Carbonate content was obtained by gasometry, elemental iron content by x ray fluorescence of sample beads, fused with sodium lithoborate.

To calculate iron flux, the following equation was used:

iron flux = SR (DBD) p

where flux is in units of $g.cm^{-2}.kyr^{-1}$ and SR = sedimentation rate (cm kyr^{-1}), DBD = dry bulk density ($g.cm^{-3}$) and p is the weight fraction of iron.

From the age model, a sedimentation rate was calculated for each sediment depth. Heavy sampling meant it was not possible to obtain a DBD value for every sample depth. Density was estimated[28] from the relationship between CO_3 content and the measured DBD of a subset of samples (14) spanning the CO_3 range. For values of p, iron(wt fraction) is estimated for every sample from the HIRM/elemental iron correlation. Dust flux was calculated from the iron (wt fraction), assuming an average iron abundance in mineral aerosols of 3.5 % [29].

1. Loubere, P. Marine control of biological production in the eastern equatorial Pacific Ocean. *Nature* **406,** 497-500 (2000).

2. Treguer P. & Pondaven, P. Silica control of carbon dioxide. *Nature* **406,** 358-359 (2000)

3. Paytan, A. Iron uncertainty. *Nature* **406**, 468-469 (2000).

4. Boyd PW *et al.* A mesoscale phytoplankton bloom in the polar Southern Ocean stimulated by iron fertilization. *Nature* **407,** 695-702 (2000).

5. Watson AJ, Bakker DCE, Ridgwell AJ, Boyd, PW & Law, C.S. Effect of iron supply on Southern Ocean CO_2 uptake and implications for glacial atmospheric CO_2. *Nature*, **407**, 730-733 (2000).

6. Coale K.H., Fitzwater S.E., Gordon R.M., Johnson KS & Barber RT. Control of community growth and export production by upwelled iron in the equatorial Pacific Ocean. *Nature*, **379**, 621-624 (1996).

7. Wells, M.L., Vallis, G.K. & Silver, E.A. Tectonic processes in Papua New Guinea and past productivity in the eastern equatorial Atlantic. *Nature*, **398**, 601-604 (1999).

8. Watson, A.J. & Lefevre, N. The sensitivity of atmospheric CO_2 concentrations to input of iron to the oceans. *Tellus*, **51B**, 453-460 (1999).

9. Lefevre, N & Watson, A.J. Modelling the geochemical cycle of iron in the oceans and its impact on atmospheric carbon dioxide concentrations. *Global Biogeochem. Cyc.*, **13**, 727-736 (1999).

10. Bareille, G., Grousset, F.E. & Labracherie, M. Origin of detrital fluxes in the southeast Indian Ocean during the last climatic cycles. *Paleoceanogr.*, **9**, 799-819 (1994).

11. Martin, J.H. Glacial-interglacial CO_2 change; the iron hypothesis. *Paleoceanogr.*, **5**, 1-13 (1990).

12. Mahowald, N. et al. Dust sources and deposition during the last glacial maximum and current climate: A comparison of model results with paleodata from ice cores and marine sediments. *J. Geophys. Res.* **104,** 15,895-15916 (1999).

13. Duce, R & Tindale, N.W. Atmospheric transport of iron and its deposition in the ocean. *Limnol. Oceanogr.* **42**, 405-418 (1991).

14. Husar, R.B., Prospero, J.M. & Stowe, L.L. Characterization of tropospheric aerosols over the oceans with the advanced very high resolution radiometer optical thickness operation product, NOAA. *J. Geophys. Res.* **102,** 16,889-16,901 (1997).

15. Measures, C.I & Vink, S. On the use of dissolved aluminium in surface waters to estimate dust deposition to the ocean. *Global Biogeochem. Cyc.*, **14**, 317-327 (2000).

16. Petit, J.R. et al. Climate and atmospheric history of the past 420 000 years from the Vostok ice core, Antarctica. *Nature*, **399,** 429-436 (1999).

17. Basile, I. et al. Patagonian origin of glacial dust deposited in East Antarctica (Vostok and Dome C) during glacial stages 2, 4 and 6. *Earth Planet. Sci. Letts.*, **146**, 573-589 (1997).

18. Diekmann, B. et al. Terrigenous sediment supply in the Scotia Sea (Southern Ocean): response to late Quaternary ice dynamics in Patagonia and on the Antarctic Peninsula. *Palaeogeog., Palaeoclimatol., Palaeoecol.*, **162**, 357-388 (2000).

19. Kumar, N. et al. Increased biological productivity and export production in the glacial Southern Ocean. *Nature*, **378**, 675-680 (1995).

20. Kidd, R.B. et al. King's Trough Flank: geological and geophysical investigations of its suitability for high-level radioactive waste disposal. *I.O.S.* Report, **166,** 1-98 (1983).

21. Reiff, J., Forbes, G., Spieksma, F. & Reynders, J. African Dust Reaching Northwestern Europe: A Case Study to Verify Trajectory Calculations. *J. Climat. & Appl. Meteorol.*, **25**, 1543-1567 (1986).

22. Jickells, T.D. & Spokes, L.J. in *The Biogeochemistry of Iron in Seawater* (eds. Turner, G. & Hunter, K.A.) (Wiley, New York, in press).

23. Martinson, D.G. et al. Age dating the orbital theory of the Ice Ages: Development of a high-resolution 0 to 300,000 years chronostratigraphy. *Quat. Res.* **27,** 1-29 (1987).

24. Shackleton, N.J. The 100,000 year ice-age cycle identified and found to lag temperature, carbon dioxide and orbital eccentricity. *Science*, **289**, 1897-1902 (2000).

25. Robinson, S.G. The late Pleistocene palaeoclimatic record of North Atlantic deep-sea sediments revealed by mineral magnetic measurements. *Phys. Earth Planet. Int.*, **42,** 22-47 (1986).

26. Maher, B.A.& Thompson, R. in *Quaternary Climates, Environments and Magnetism* (eds. Maher, B.A. & Thompson, R.) 1-48 (Cambridge University Press, UK) (1999).

27. Chapman, M.R. & Shackleton, N.J. Millenial-scale fluctuations in North Atlantic heat flux during the last 150,000 years. *Earth Planet. Sci. Letts.* **159,** 57-70 (1998).

28. Hovan, S.A., Rea, D.K. & Pisias, N.G. Late Pleistocene continental climate and oceanic variability recorded in Northwest Pacific sediments. *Paleoceanogr.*, **6,** 349-370 (1991).

29. Duce, R.A. in *The Role of Air-Sea Gas Exchange in Geochemical Cycles* (ed. Buat-Menard, P.) (Reidel, Dordrecht) 1986.

30. DeMenocal, P.B., Ruddiman, W.F. & Pokras, E.M. Influences of high-latitude and low-latitude processes on African terrestrial climate – Pleistocene eolian records from Equatorial Atlantic-Ocean Drilling Program Site-663. *Paleoceanogr.*, **8**, 209-42 (1993).

31. Petit, J.R. Personal communication.

Acknowledgements
We are grateful to Southampton Oceanography Centre for allowing sampling of Core 82PCS01, Katy Miller for picking the foraminifera, Sarah Dennis and Gregg McIntosh for performing oxygen isotope and magnetic analyses, respectively, and an anonymous referee for their thoughtful and constructive review.

Correspondence and requests for materials should be addressed to B. Maher (b.maher@lancaster.ac.uk).

Figure legends. Figure 1 The high-resolution foraminiferal (*Globorotalia bulloides)* oxygen isotope record for Piston Core 82PCS01 (42^{o}05'N 23^{o}31'W, water depth 3540 m). The chronology is based on the indicated tie points between the measured data and the orbitally-tuned deep sea record of Martinson et al.[23]. The oxygen isotope substages are marked on the tie lines. The Vostok δ^{18}O (in air)[16] is plotted using the GT4 timescale. For the 100 - 170 ka period represented by these records, the chronology is in excellent agreement with an independent age model based on orbital tuning of both the marine and Vostok records to tilt and precession cycles[24].

Figure 2 Oxygen isotope and dust (HIRM and terrigenous %) records from the eastern N. Atlantic. a) Oxygen isotope data for Piston Core 82PCS01, 8.8m of carbonate ooze interbedded with marly ooze; b) oxygen isotope data for Ocean Drilling Program Hole 633 [30], from the eastern tropical Atlantic (1.2 ^{o}N 11.9 ^{o}W); c) HIRM data for Core 82PCS01; d) published terrigenous % values for ODP Hole 663 [30]. The vertical line represents Termination II at ~130 ka[23].

Figure 3 Dust, isotopic and CO_2 records from the N. Atlantic and the Vostok ice core. a) Dust flux values for Core 82PCS01; b) dust flux values for the Vostok ice core[16,31]; c) dust concentration in the Vostok ice core [16]; d) oxygen isotope data for Piston Core 82PCS01; d) oxygen isotope data for the Vostok ice core[16]; e) oxygen isotope data (in air) in the Vostok ice core[16]; f) deuterium data for the Vostok ice core [16]; g) CO_2 data for the Vostok ice core [16]. The vertical lines at 137 ka and 130 ka mark the onset of the CO_2 rise recorded at Vostok (137 ka) and the Termination II boundary (130 ka).

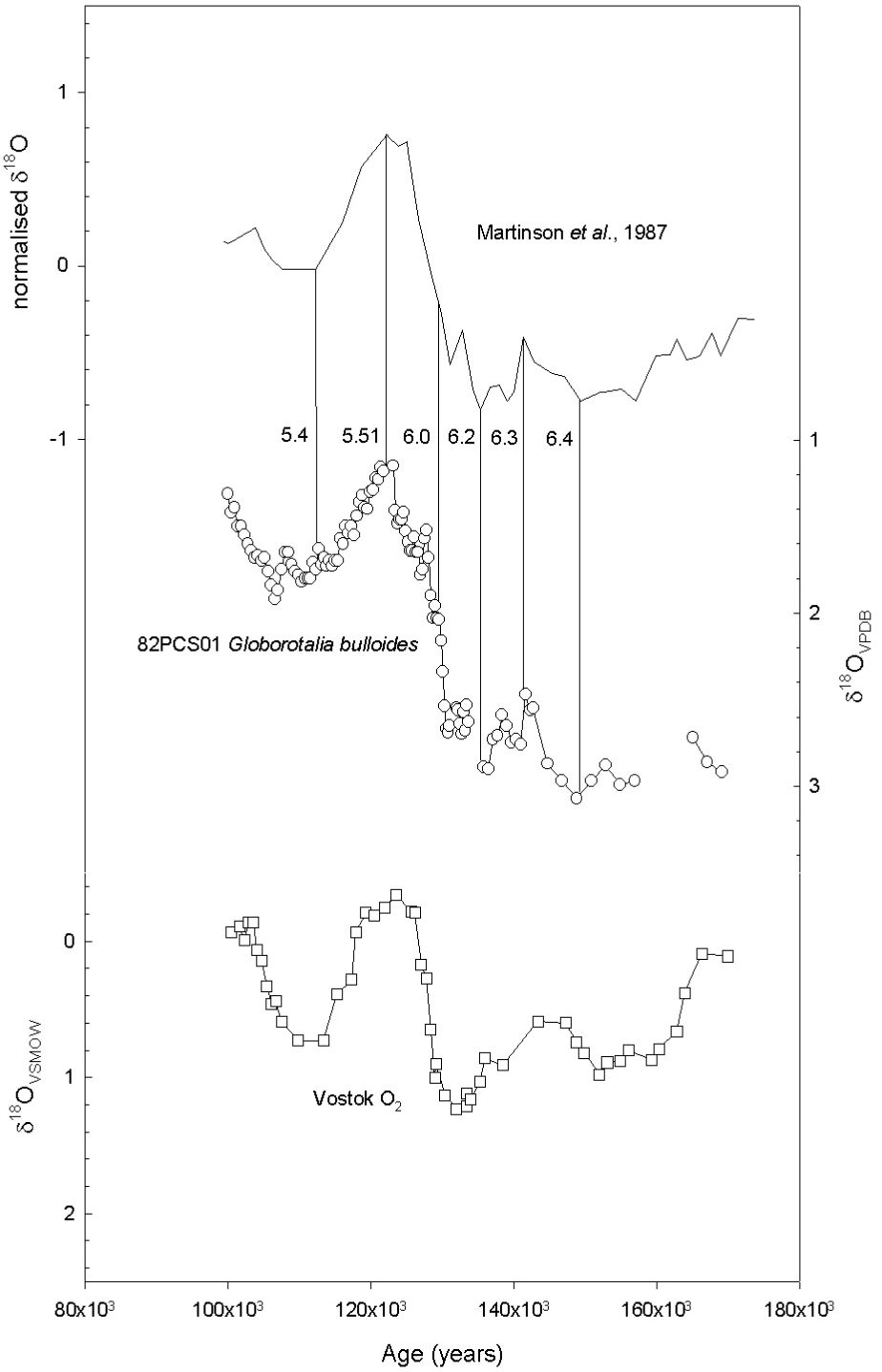
normalised $\delta^{18}O$
1
0
-1
Martinson *et al.*, 1987
5.4
5.51
6.0
6.2
6.3
6.4
82PCS01 *Globorotalia bulloides*
1
2
3
$\delta^{18}O_{VPDB}$
0
1
2
$\delta^{18}O_{VSMOW}$
Vostok O_2
80x10³
100x10³
120x10³
140x10³
160x10³
180x10³
Age (years)

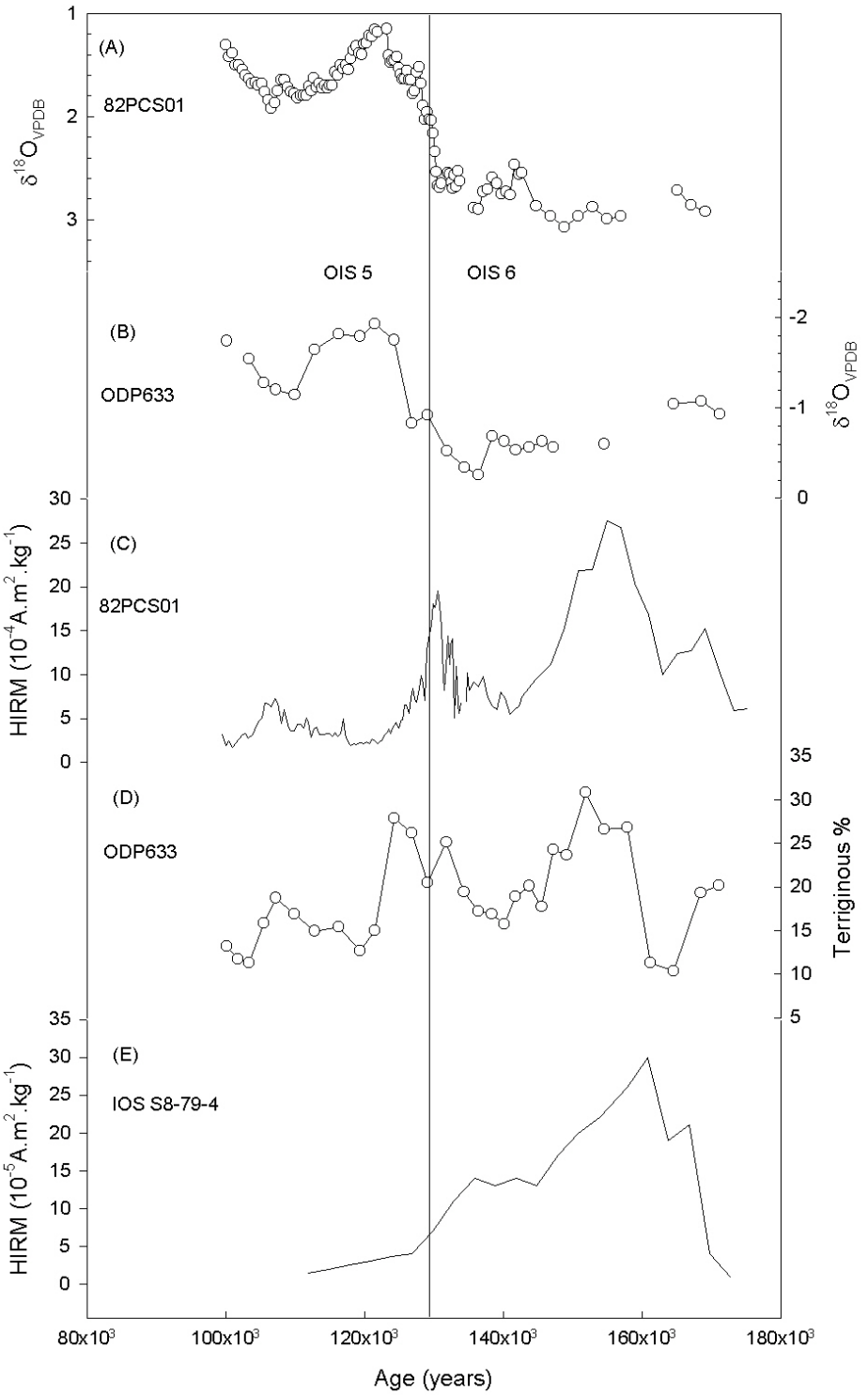
(A)
82PCS01
$\delta^{18}O_{VPDB}$
OIS 5
OIS 6
(B)
ODP633
$\delta^{18}O_{VPDB}$
(C)
82PCS01
HIRM (10^{-4}A.m^2.kg^{-1})
(D)
ODP633
Terriginous %
(E)
IOS S8-79-4
HIRM (10^{-5}A.m^2.kg^{-1})
80x10^3
100x10^3
120x10^3
140x10^3
160x10^3
180x10^3
Age (years)

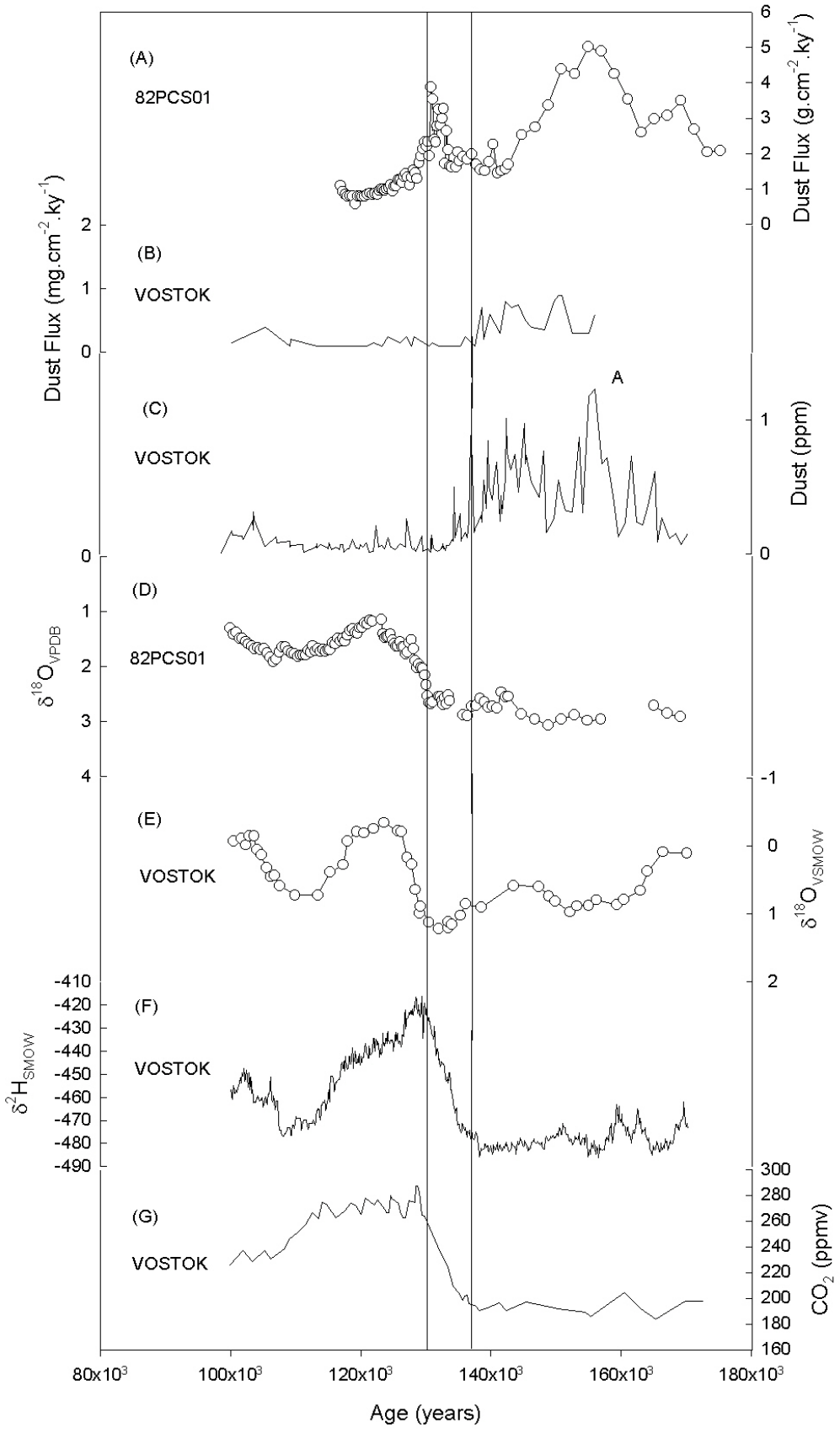
(A)
82PCS01
Dust Flux (g.cm-2.ky-1)
(B)
VOSTOK
Dust Flux (mg.cm-2.ky-1)
(C)
VOSTOK
A
Dust (ppm)
(D)
82PCS01
δ18OVPDB
(E)
VOSTOK
δ18OVSMOW
(F)
VOSTOK
δ2HSMOW
(G)
VOSTOK
CO2 (ppmv)
80x10³
100x10³
120x10³
140x10³
160x10³
180x10³
Age (years)